The Millimeter-wave Bolometric Interferometer

S. Ali[1], P. A. R. Ade[2], J. J. Bock [3], G. Novak[4], L. Piccirillo[2], P. Timbie[1], G. S. Tucker[5]

[1]Dept. of Physics, University of Wisconsin—Madison, Madison, WI 53706

[2]Dept. of Physics and Astronomy, University of Wales—Cardiff, Cardiff CF243YB, Wales, UK

[3]Jet Propulsion Laboratory, Pasadena, CA 91109

[4]Department of Physics and Astronomy, Northwestern University, Evanston, IL 60208

[5]Dept. of Physics, Brown University, Providence, RI 02912

The Millimeter-wave Bolometric Interferometer (MBI) is a proposed ground-based instrument designed for a wide range of cosmological and astrophysical observations including studies of the polarization of the cosmic microwave background (CMB). MBI combines the advantages of two well-developed technologies — interferometers and bolometric detectors. Interferometers have many advantages over filled-aperture telescopes and are particularly suitable for high resolution imaging. Cooled bolometers are the highest sensitivity detectors at millimeter and sub-millimeter wavelengths. The combination of these two technologies results in an instrument with both high sensitivity and high angular resolution.

1. INTRODUCTION

Astrophysical observations are almost always limited by wavelength, angular resolution and/or sensitivity constraints. The Millimeter-wave Bolometric Interferometer (MBI) combines the high angular resolution of interferometers with the sensitivity of bolometers. The result is a proposed new instrument suitable for a wide range of cosmological and astrophysical observations. MBI will have a large baseline ($\sim$ 6 m) and will probe sub-arcminute angular scales. A prototype of this instrument, MBI-B, is a small baseline ($\sim$ 0.14 m) version of MBI designed to search for B-mode polarization in the CMB at degree angular scales.

With the large baseline MBI it should be possible to address the following scientific goals:

- Characterize the polarization of the CMB. MBI will measure simultaneously the temperature and polarization anisotropy of the CMB at angular scales from $30'$ to $40''$.
- Characterize clustering in the far-infrared background (FIRB).
- Measure and map magnetic fields near the center of the galaxy by measuring the Faraday rotation of synchrotron radiation.
- Measure the wavelength dependent properties of dust polarization.
- Image the Sunyaev-Zeldovich (SZ) effect in clusters of galaxies.
- Spectrally separate the kinetic and thermal SZ effects.
- Search for CMB and SZ point source foregrounds.

MBI will serve as a testbed for a possible future space-based interferometer mission to measure the polarization of the CMB. The angular resolution of space telescopes is normally limited by the aperture size which can fit in a rocket fairing. An interferometer can overcome this size limitation, by using an optical bench which extends after launch.

MBI-B will be constructed first to demonstrate the MBI concept. It's goals are to:

- Search for primordial B-mode polarization in the cosmic microwave background (CMB).
- Search for intracluster magnetic fields via Faraday rotation.
- Map magnetic fields near the core of our galaxy.

The main characteristics of MBI-B and MBI are presented in Table 1. The field-of-view (FOV) of each interferometer element is denoted by θ and the size of the synthesized beam size by ϕ.

TABLE 1: MBI Characteristics and Sensitivity.

λ	MBI-B 20×20 array		MBI-B		MBI	
	Sensitivity	Days to reach	θ	ϕ	θ	ϕ
(mm)	(mK$\sqrt{\mathrm{s}}$)	3 μK/sky pixel	(degrees)	(degrees)	(arcmin)	(arcmin)
3	0.6 (1.1)	0.5 (1.4)	7	1.4	10	2.0
2	0.7 (1.3)	0.6 (2.2)	7	1.4	7.2	1.4
1	2.9 (5.4)	11. (37.)	7	1.4	3.6	0.7

Calculations assume equivalent temperature of atmosphere, optics and CMB is 40 K.
Each interferometer views 25 pixels on the sky simultaneously.
The sensitivity is the sensitivity for each sky pixel to fluctuations in a 2.7 K blackbody.
Sensitivity numbers and integration times are for background-noise-limited and,
   in parentheses, (detector-noise-limited) cases.

2. SCIENCE

2.1 CMB Polarization: Both the temperature anisotropy and spectral information of the CMB strongly constrain cosmological models, but there is another component — the *polarization* of the CMB — which has not yet been detected. In most models the amount of this polarization is $\leq 10\%$ of the temperature anisotropy (Bond & Efstathiou 1987). The fundamental nature of the prediction is such that the mere detection of polarization of roughly the correct amplitude would have great significance. Because the size of the expected polarization signal is so small, it is necessary to use the highest sensitivity detection scheme possible while simultaneously controlling and minimizing potential systematic effects.

Polarization on the sky may alternatively be separated into "electric" (E) and "magnetic" (B) components (Hu & White, 1997; Seljak & Zaldarriaga 1998; Kamionkowski et al. 1997). E and B multipole patterns are, respectively, gradient and curl decompositions of the polarization pattern, much like Q and U, but more directly related to the source generation mechanism. E type polarization is generated by scalar or tensor perturbations at the time of last scattering, while B type polarization is only produced by tensor perturbations and cannot be produced by scalar perturbations due to parity conservation. As a result a search for B mode polarization is a direct search for tensor modes in the early universe. The signal for B type polarization peaks up at degree angular scales.

For a noise-limited experiment the best observation strategy for detecting B-mode polarization is to spend more observation time on a restricted part of the sky rather than to survey a large part of the sky (Jaffe et al. 2000). A beam size smaller than $\sim 1°$ does not significantly improve the sensitivity to detecting B-mode polarization. At a wavelength of 2 mm MBI-B has a FOV of $\sim 7°$ and an effective resolution of $1.2°$. This choice of FOV and resolution represents a trade-off to most effectively probe the B-mode polarization signal. Figure 1 illustrates the trade-off between survey size and angular resolution and shows the choice of instrument parameters for MBI-B is nearly optimal.

The higher angular resolution of MBI is chosen to measure the CMB polarization power spectrum at smaller angular scales where the signal from acoustic oscillations is expected to appear. The expected polarization power spectrum at small scales is closely related to the temperature power spectrum at these scales.

2.2 Galactic Studies: MBI-B and MBI can also be used, for example, to measure the wavelength dependent polarization properties of dust. Observations of the thermal component of the dust radiation have revealed that the wavelength-dependence of the polarization is surprisingly strong. The observations are few, and are specifically limited to molecular cloud envelopes, but they give a consistent picture of a degree of polarization that falls with wavelength in the far-infrared,
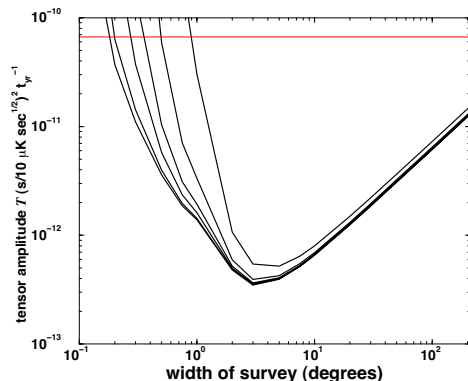
Figure 1. The smallest tensor amplitude that could be detected at 3σ with an experiment with a detector sensitivity of 10 $\mu K\sqrt{s}$ that observed for one year and maps a square region of sky of given width. The result scales with the square of the detector sensitivity and inversely with the duration of the experiment. The curves are (from top to bottom) the FWHM beamwidths of 1.0, 0.5, 0.3, 0.2, 0.1 and 0.05 degrees. The horizontal line shows the upper limit to the tensor amplitude from COBE. MBI-B will improve the COBE measurement by more than a factor of 10. (Reproduced from Jaffe et al. 2000.)

and then begins to rise in the submillimeter, near 350 μm wavelength. These results have been explained using a model in which the efficiency of grain alignment is correlated with exposure to radiation from both embedded stars and external sources (Hildebrand et al. 1999). The importance of understanding the physics of grain alignment lies principally in the fact that studies of polarized dust emission provide one of the few methods for mapping magnetic fields, especially in the dense regions where stars form. Without the physical understanding it is difficult to determine, for any given line-of-sight, which specific regions are being sampled, within an extended, heterogeneous and complex molecular cloud.

3. THE ADDING INTERFEROMETER

In a simple 2-element radio interferometer, signals from two telescopes aimed at the same point in the sky are multiplied (correlated) so that the sky temperature is sampled with an interference pattern with a single spatial frequency. In an interferometer that uses incoherent detectors, such as an optical interferometer, the electric field wavefronts from two telescopes are added and then squared in a detector — an "adding" interferometer as opposed to a "multiplying" interferometer (Rohlfs 1996). See Figure 2. The adding interferometer recovers the same visibility as a multiplying interferometer.

4. WHY USE A BOLOMETRIC INTERFEROMETER?

While inteferometers and bolometers are each highly developed, to our knowledge, no instrument which combines these two powerful technologies has ever been built. There are a number of advantages achieved in combining the two technologies, which we now describe.

For measurements which require high angular resolution, large single dishes are often impractical for a number of reasons including mass, deformations due to gravity and cost. Interferometers effectively enable high angular resolution by reproducing the resolution performance of a large dish; the trade-off is a reduction in collection area if the interferometer area is not filled. The limit of a filled interferometer is a single large dish. Thus for equivalent angular resolution, an interferometer can be substantially simpler and less costly than a single large aperture.

4.1 Better angular resolution for equivalent size. For a monolithic dish of diameter equal to the length of a two-element interferometer baseline, the interferometer has angular resolution
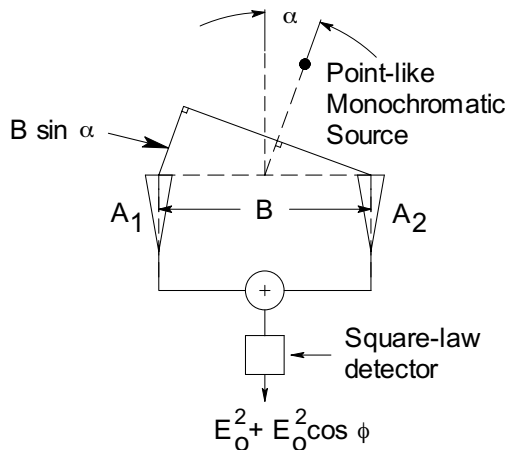
Figure 2. Adding interferometer. At antenna A_2 the electric field is E_0, and at A_1 it is $E_0 e^{i\phi}$, where $\phi = kB \sin \alpha$ and $k = 2\pi/\lambda$. B is the length of the baseline, and α is the angle of the source with respect to the symmetry axis of the baseline, as shown. (For simplicity consider only one wavelength, λ, and ignore time dependent factors.) In a multiplying interferometer the in-phase output of the correlator is proportional to $E_0^2 \cos \phi$. For the adding interferometer, the output is proportional to $E_0^2 + E_0^2 \cos \phi$. Modulation of the length of the baseline allows phase-sensitive detection to recover both the in-phase and quadrature phase interference terms and reduces susceptibility to low-frequency drifts ($1/f$ noise) in the bolometer and readout electronics.

roughly twice as good as that of the monolithic dish. The reason for this difference in angular resolution is the following: For acceptable sidelobe performance, the edge illumination of the monolithic dish must be tapered considerably, which reduces the effective aperture diameter. The effective edge taper of the interferometer is much smaller, so the effective diameter is nearly equal to the length of the baseline. The sidelobe rejection of an interferometer can also be significantly better than that from a single dish.

4.2 No chopping and scanning. Single dishes with either coherent or incoherent detectors typically use some form of "chopping" which is achieved either by nutating a secondary mirror or by steering the entire primary at a rate faster than the $1/f$ noise in the atmosphere and detectors. Similar approaches are used with arrays of detectors. Since an interferometer does not require this rapid chopping, the time constants of the bolometers used can be relatively long.

Interferometers provide direct 2D imaging and do not require scanning strategies; in addition individual maps may be mosaiced. Since beam steering is not required in an interferometer, for ground-based observations the signal from an interferometer is also significantly less affected by the atmosphere (Church 1995, Lay & Halverson 2001).

4.3 Multiplex advantage. For n apertures there are $n(n-1)/2$ baselines. The n beams can be combined in $n(n-1)/2$ pairs. However, the n beams can also be combined into a single beam, which results in a multiplexing advantage. There are two advantages to multiplexing. First, since the photon signal-to-noise ratio is increased, lower sensitivity detectors can be used. Second, by having all beams traverse symmetric paths, unmeasured path changes in the optics due to temperature variations, for example, are minimized. In order to accomplish multiplexing, each pair of telescope beams must be modulated at a unique frequency so the signal from telescope pairs can be recovered. With an array of N_D detectors, there is also an increase in observation speed since there are now effectively many interferometers operating simultaneously.

5. INSTRUMENT

The basic optical designs of the MBI-B and MBI are shown in Figure 3. They are each "Fizeau" or "image-plane" interferometers (as opposed to "Michelson" interferometers such as the proposed SPECS instrument described in Mather et al. (2000), Leisawitz et al. (2002) and Zhang et al. (2001)). The optical design has a number of desirable features. The interferometer elements

do not move with respect to one another which reduces systematic effects. Potential systematic effects are reduced through multiple levels of switching. The sky flats are translated sinusoidally by several wavelengths at a low frequency (< 1 Hz); the effective switching frequency is higher than that of the small mechanical motion. The entire interferometer can be rotated about the optical axis at a rate of $\sim 5°$/s.

MBI will build on MBI-B by providing a long baseline and thus much higher angular resolution. The concept for MBI is shown in Figure 4. The platform is similar to MBI-B in that it has altitude-azimuth-theta axes, but the baseline is much larger (~ 6 m).
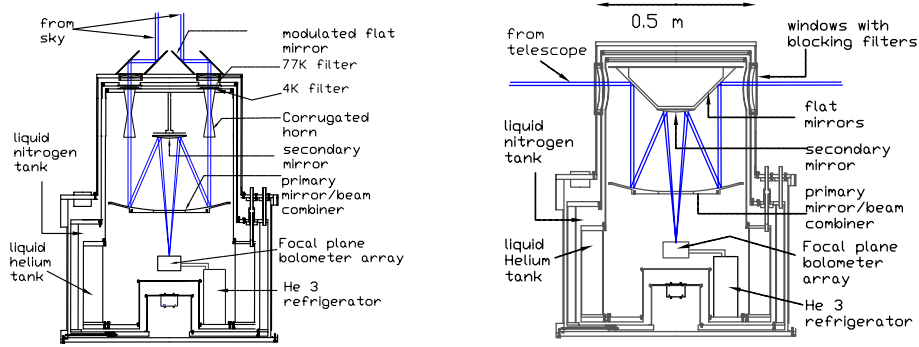
Figure 3. The MBI-B (left) and MBI (right) optical design. In the MBI-B design light from the sky is first reflected from two flat mirrors at $45°$. One of each pair of flat mirrors is modulated by a few wavelengths at a unique low frequency. Light enters the cryostat from the top, passing through blocking filters. The interferometer beams are defined with back-to-back corrugated feed horns; for clarity only two horns are shown. The beams are combined with a primary and secondary mirror in a Cassegrain telescope configuration. The interference pattern is imaged by a bolometer array in the focal plane. The bolometer array is cooled to below 0.3 K with a [3]He refrigerator. The MBI design is similar to the MBI-B design except that light enters the side of the cryostat and strikes a flat mirror at $45°$. The light comes from Cassegrain telescopes located up to several meters away. With only minor modifications the MBI-B receiver can be used for the MBI.

5.1 Bandwidth. While the sensitivity of a receiver to broadband signals increases as the square root of the bandwidth, for interferometers, the bandwidth restricts the angular range, θ, over which fringes are detected (Thompson, Moran & Swenson 1998; Boker & Allen 1999). If we assume the path lengths for a source at the center of the field of view (FOV) are equal, then the path length difference for a source at an angle θ from the center along the baseline axis is θB, where B is the baseline distance. If this path length difference is small compared to the coherence length of the light $\lambda^2/\Delta\lambda$, then the fringe contrast is not affected. Thus the FOV is determined by $\theta_{FOV} \leq (\lambda/\Delta\lambda)(\lambda/B)$. This equation indicates that for angles of the order of the product of the spectral resolution times the angular resolution, the fringe smearing is important. This relation imposes restrictions on the ratio between the maximum baseline achievable by the interferometer and the spectral bandwidth of the receiver. A choice of 20% spectral bandwidth will set the maximum baseline to about 5 times the diameter of each single telescope.

5.2 Sensitivity. Here we make an estimate for the expected sensitivity of MBI-B. These calculations are the basis for the projected sensitivity figures in Table 1.

MBI-B is an example of a Fizeau, or image-plane interferometer. Two main methods have been studied for combining the beams from the n different apertures in such an instrument (Prasad & Kulkarni 1989, Roddier & Ridgway 1999, Nakajima & Matsuhara 2001, Nakajima 2001). In one scheme, the ${}^nC_2$ interferometer, the radiation entering each aperture is divided $n-1$ ways and combined pairwise with the power from each of the other apertures to form an interference pattern on an array of detectors; there is one detector array for each of the $n(n-1)/2$ baselines. In
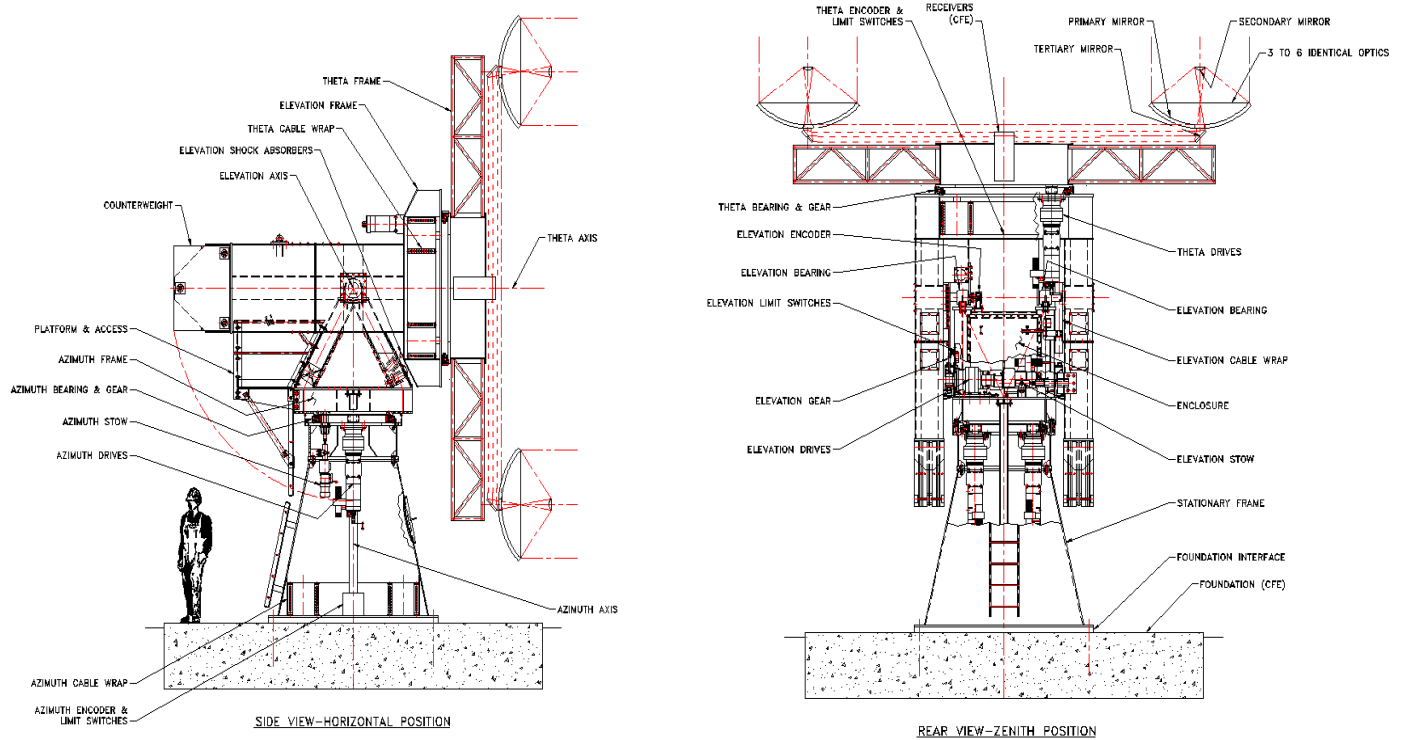
Figure 4. Concept for MBI (side and rear views). MBI will have eight 1.2 m telescopes with a maximum baseline of 6 m; for clarity only two telescopes are shown here. The telescopes are attached to a circular platform which can rotate about the optical axis — denoted here as the "theta" axis. The cryogenic beam combiner and receiver is located at the center of the circular platform. The platform is fully steerable in altitude and azimuth.

the second method, the ^nC_n interferometer, all n beams are combined simultaneously on a single 2-dimensional array of detectors. In the case where the sensitivity of the detectors is limited only by the photon-noise from the background radiation all forms of beam combination produce approximately the same sensitivity (Prasad & Kulkarni 1989). We have chosen the latter (^nC_n) approach because it is extremely simple to combine the n beams by bringing them to a focus in the focal plane of a telescope. No beam splitters are required. We locate the beam-combining telescope in a cryostat and cool the bolometer array in its focal plane to sub-Kelvin temperature. The array of bolometers can be considered as a multipixel correlator. A total of $n_c = n(n-1)/2$ fringe patterns or interferograms (one for each baseline) are superposed on this array in a "criss-cross" pattern. Each interferogram contains $2(\theta/\phi)$ fringe cycles, where θ is the primary antenna beam and ϕ is the resolution of the image corresponding to the maximum baseline. A total of $4(\theta/\phi)$ detector pixels are required along one dimension of the array for Nyquist sampling. Hence, a two-dimensional detector array must have a minimum of $N_D = 16(\theta/\phi)^2$ elements. Additional detectors do not provide any improvements in sensitivity.

For MBI-B full sampling of the interference plane requires $N_D = 400$. The detectors are single-mode polarization-sensitive bolometers (Turner et al. 2001), which will initially operate at a wavelength of 2 mm with a 20% bandwidth and optical efficiency $\eta = 0.3$. The ultimate sensitivity per detector pixel is achieved when the intrinsic bolometer noise is equal to or less than the statistical fluctuations of the background noise, the so called BLIP condition. We assume the optical loading on the bolometers is equal to the sum of the power loading from the optics, atmosphere and the CMB. At White Mountain, CA (altitude = 3800 m), for observations at a wavelength of 2 mm and at an observing angle $30°$ from the zenith, the effective temperature of the atmosphere is about 40 K (Grossman 1989). To calculate the Noise Equivalent Temperature

(NET), we divide the BLIP by $dB(T)/dT$ calculated for a blackbody at 2.735 K to arrive at an estimated estimated NET of $\sim 548\ \mu K\sqrt{s}$, equivalent to a system noise temperature of about 67 K.

The expression for sensitivity for a direct detector interferometer depends on whether the detectors are limited by detector noise or by background photon noise. In all cases we assume that the interference pattern in the focal plane is fully sampled with N_D detectors according to the prescription above.

In the detector-noise-limited case, we obtain $\delta T = (T_s/\sqrt{\Delta\nu\Delta\tau 2n_c})(\theta/\phi)^2$ where $\Delta\nu$ is the optical bandwidth of the detectors, $\Delta\tau$ is the integration time, and the other quantities are as defined above. This expression is identical to that for a radio interferometer (Partridge 1995). δT is the noise in each pixel in the recovered image of the sky; the interferometer observes $(\theta/\phi)^2$ such sky pixels simultaneously. The expression is the same as that for a filled aperture, total power receiver with one detector and one pixel (of angular size ϕ) on the sky except for the factor of $(\theta/\phi)^2/\sqrt{2n_c}$. This factor accounts for the reduction in sensitivity arising because the interferometer array is not a completely filled aperture. For an interferometer with baseline length B and n apertures each of diameter D, $(\theta/\phi)^2/\sqrt{2n_c} \sim (B/D)^2/n$, which is the inverse of the aperture filling factor, q.

In the case of an interferometer in which the detectors are background-noise-limited the sensitivity scales as one over the square root of the aperture filling factor. As the filling factor is reduced, the signal reaching the detector array decreases linearly with q, but the photon noise on each detector decreases by the square root of q; the signal to noise is degraded as $\sqrt{q}$. Hence, in this case $\delta T = (T_s/\sqrt{\Delta\nu\Delta\tau n})(\theta/\phi)$ (Roddier & Ridgway 1999).

For MBI-B we have $n = 8$, so $n_c = 28$ at a single wavelength (2 mm). To measure these baselines fully, MBI-B requires $N_D = 20 \times 20 = 400$ bolometers in the array; it will observe a total of $(\theta/\phi)^2 = 25$ pixels on the sky simultaneously. In the detector-noise-limited case with $N_D = 400$ the noise per sky pixel in the synthesized image is then $\delta T = 1.3\ mK\sqrt{s}$. The time required to integrate this image down to 3 μK noise per sky pixel is $(\delta T/3\,\mu K)^2 = 2.2$ days.

According to Jaffe et al. (2000), a measurement at this sensitivity level with MBI-B's angular resolution and field-of-view can constrain the amplitude of the tensor modes (gravitational waves) created during inflation. The quantity of interest is the tensor-to-scalar mode ratio; with the parameters described here MBI-B will improve on the T/S ratio established by COBE by over a factor of 10.

This test of the MBI-B concept will observe in only one wavelength band at a time. The band is defined by an inductive-capacitive mesh filter placed in front of the array. In a future version of MBI-B, multiple bands could be observed simultaneously by using dichroic beamsplitters or frequency-selective-bolometers (Kowitt et al. 1996).

6. SUMMARY

We have outlined a concept for an adding interferometer that uses bolometer arrays for precision measurements in astrophysics and observational cosmology. We plan to construct a short baseline interferometer (MBI-B) to evaluate the design and use it to search for the extremely faint B-modes that are anticipated in the CMB at degree angular scales. Later, this same beam combiner/detector system could be coupled to an array of reflectors with $\sim$6 m baselines to explore smaller angular scales. Both of these instruments could serve as prototypes for more ambitious space-based interferometers.

7. REFERENCES

Boker T & Allen, J. A., "Imaging and Nulling with the Space Interferometer Mission", ApJSS, 125, 123 (1999)

Bond, J. R. & Efstathiou, G. "Microwave Anisotropy Constraints on Isocurvature Baryon Models," MNRAS, 226, 655 (1987)

Church, S.E., "Predicting residual levels of atmospheric sky noise in ground-based observations of the Cosmic Background Radiation," MNRAS, 272, 551 (1995)

Grossman, E. Airhead Software Inc., Boulder CO (1989)

Hildebrand, R. H. et al. "The Far-Infrared Polarization Spectrum: First Results and Analysis," ApJ, 516, 834 (1999)

Hu, W. & White, M. "A CMB Polarization Primer," New Astronomy, 2, 323 (1997)

Jaffe, A. H., Kamionkowski, M. & Wang, L. "A Polarization Pursuer's Guide," PRD, 61, 083501 (2000)

Kamionkowsi, M., Kosowsky, A. & Stebbins, A. "A Probe of Primordial Gravity Waves and Vorticity," PRL, 78, 2058 (1997)

Kowitt, M. S., Fixsen, D. J., Goldin, A. & Meyer, S. S. "Frequency Selective Bolometers," Appl. Opt., 35, 5630 (1996)

Lay, O. P. & Halverson, N. W. "The Impact of Atmospheric Fluctuations on Degree-Scale Imaging of the Cosmic Microwave Background," ApJ, 543, 787 (2001)

Leisawitz, D. et al. "Probing the Invisible Universe: The Case for Far-IR/Submillimeter Interferometry, " Proceedings of the Second Workshop on New Concepts for Far-Infrared and Submillimeter Space Astronomy, University of Maryland, March 7–8, 2002

Mather, J. C., Moseley, S. H., Leisawitz, D., Zhang, X., Dwek, E. Harwit, M., Mundy, L. G., Mushotzky, R. F., Neufield, D., Spergel, D. & Wright, E. L. "The Submillimeter Probe of the Evolution of Cosmic Structure," submitted to the Review of Scientific Instruments (2000)

Nakajima, T. "Sensitivity of a Ground-based Infrared Interferometer for Aperture Synthesis Imaging," P. A. S. P., 113, 1289 (2001)

Nakajima, T. & Matsuhara, H. "Sensitivity of an imaging space based interferometer," Applied Optics, 40, 514 (2001)

Partridge, R. B. "3K: The Cosmic Microwave Background Radiation," New York: Cambridge University Press (1995)

Prasad, S. & Kulkarni, S. R. "Noise in Optical Synthesis Images I. Ideal Michelson Interferometer," J. Opt. Soc. Am. A, 6(11), 1702 (1989)

Roddier, F. & Ridgway, S. T. "Filling Factor and Signal-to-Noise Ratios in Optical Interferometric Arrays," P. A. S. P., 111, 990 (1999)

Rohlfs, K. & Wilson, T. L., Tools of Radio Astronomy, 2nd ed., Springer, New York (1996)

Seljak, U. & Zaldarriaga, M. "Polarization of the Microwave Background: Statistical and Physical Properties," in "Fundamental Parameters in Cosmology," proceedings of the XXXIIIrd Recontres de Moriond (1998)

Thompson, A. R., Moran, J. M. & Swenson, G. W. Jr. "Interferometry and Synthesis in Radio Astronomy," Krieger Publishing Company, Malabar, Florida (1998)

Turner, A. D., Bock, J. J., Beeman, J. W., Glenn, J., Hargrave, P. C., Hristov, V. V., Nguyen, H. T., Rahman, F., Sethuraman, S., and Woodcraft, A., "Silicon Nitride Micromesh Bolometer Array for Submillimeter Astrophysics," Appl. Opt. 40(28), 4921 (2001)

Zhang, X., Feinberg, L., Leisawitz, D., Leviton, D. B., Martino, A. J. & Mather, J. C. "The Wide-Field Imaging Testbed," IEEE Aerospace Conference Proceedings, 3, 1453 (2001)